Journal of Combinatorial Mathematics
and Combinatorial Computing
www.combinatorialpress.com/jcmcc

Combinatorial Press

Study of real-time control in the optimization of human specimen fluid exchange process using gradient descent algorithm in adaptive regulation mode

Li Xu[1,✉], Xiuli Wang[1], Ke Wang[2]

[1] *Medical College, Shandong Yingcai University, Jinan, Shandong, 250104, China*

[2] *Shandong Weiping Information Security Assessment Technology Co., Ltd., Jinan, Shandong, 250101, China*

ABSTRACT

The human specimen, due to its non-renewable nature, requires the liquid exchange process in adaptive regulation mode to realize precise control. In this paper, a stochastic parallel perturbation-based gradient descent algorithm (SPGD) is introduced into the real-time control system for human specimen liquid exchange. The SPGD algorithm is used to assist the real-time control system to monitor the liquid concentration and regulate the liquid exchange power in real time, so as to keep the liquid exchange speed fast and stable and reduce the risk of specimen damage. The advantages of SPGD algorithm and real-time control system in the process of human specimen liquid exchange are verified through several experiments. The results show that there is a correlation between different liquid concentrations, real-time power and liquid exchange speed, and the combination of SPGD algorithm and real-time monitoring of the changes between the three can improve the stability of liquid exchange. The SPGD algorithm with the introduction of stochastic parallel perturbations reaches an evaluation function value of 0.83 at 31 iterations and a convergence accuracy of 0.9698 after 150 iterations. The convergence speed and accuracy are better than the unimproved SPGD algorithm. During the real-time control process, the relative error of pipetting is not more than 1.5%, and the repeatability deviation is less than 1%. Within the time range of 0-120ms, the real-time control system introducing SPGD algorithm can give the changing power of liquid exchange, which guarantees the specimen safety in the process of liquid exchange.

Keywords: adaptive regulation, SPGD algorithm, stochastic parallel perturbation, human specimen fluid exchange, real-time control

✉ Corresponding author.
E-mail address: dingluo825@126.com (L. Xu).
Received 20 February 2024; Revised 25 April 2024; Accepted 20 November 2024; Published Online 16 April 2025.
DOI: 10.61091/jcmcc127b-331
© 2025 The Author(s). Published by Combinatorial Press. This is an open access article under the CC BY license (https://creativecommons.org/licenses/by/4.0/).

1. Introduction

Human specimens are an important and indispensable tool in medical education, scientific research and forensic identification, and they have been carefully handled to be preserved for a long period of time and serve for teaching, research and exhibition. Usually, human specimens in the frozen environment can not meet the long-term preservation requirements, so immersion preservation is a common method, whether for organs, human tissue research, cadaver preservation, etc. need to be immersed in preservation fluid, to prevent the cells from swelling, mildew, deterioration, decay [1-3]. In the preservation of human specimens, due to the different types of specimens and preservation methods, the specimens need to be regularly changed liquid work, which is an important process to ensure the long-term stability of human specimens [4-5]. However, the preservation fluid in the preservation liquid preservation liquid (such as formalin liquid) may have toxicity, which is hazardous to human health, resulting in a high risk and low efficiency of the fluid change process [6]. And there are roughly six steps in the specimen fluid exchange process: wearing protective equipment, confirming the specimen information; removing the old culture fluid to avoid liquid spills; gently rinsing the specimen to remove the residual old fluid; adding an appropriate amount of new culture fluid to ensure adequate coverage of the specimen; resealing the container, recording the time of the fluid exchange with the operator; and observing the state of the specimen and adjusting the environmental conditions according to the requirements [7-8]. It seems to be a simple process of fluid exchange, but in practice, the efficiency of large-scale fluid exchange is significantly reduced. Therefore, fluid exchange systems were developed and applied to solve the problems of low efficiency and safety. However, due to the different states of specimens, with differences in environmental requirements (e.g., temperature, CO2 concentration) and fluid quality (deterioration, viscosity), dynamic fluid exchange requirements are difficult to be realized in traditional fluid exchange systems because the fixed state of the threshold setting is extremely poorly adapted to the dynamic requirements, which is often reliant on past experience and does not take into account the state of the specimen at the moment [9-10]. For the stability of human specimens, the development of a dynamic environment for real-time control of fluid exchange scheme is of great research importance.

As a basic tool in the field of optimization, the gradient descent algorithm uses the negative gradient direction to determine a new search direction for each iteration, enabling each iteration to gradually reduce the loss function to be optimized [11]. It is widely used in machine learning, deep learning, and all kinds of numerical computation scenarios to optimize the parameters or weights of the model and improve the accuracy of the model, and at the same time, it can optimize the stability of the process by combining with other methods in the dynamic process, which is advantageous in large-scale and high-dimensional optimization events [12-15].

In this paper, we analyze the method of fluid exchange of specimen bottles and the principle of automatic fluid exchange, etc., to clarify the process and steps of fluid exchange. A gradient descent algorithm is chosen to be introduced into the real-time control system in adaptive regulation mode to calculate the real-time liquid concentration and the corresponding power changes. The limitations of the gradient descent algorithm are optimized using stochastic parallel perturbation and the SPGD algorithm is designed. The liquid concentration and real-time power sample sets are constructed to improve the learning and output capability of the SPGD algorithm and enhance the real-time power monitoring effect. The gradient descent algorithm before and after optimization is simulated and compared experimentally to determine the convergence advantage of the optimized SPGD algorithm. Further analyze the error of the real-time control system introduced SPGD algorithm in the pipetting step. Combined with practical applications to prove the ability of the real-time control system introducing SPGD algorithm to reduce the risk of liquid exchange.

2. Analysis of technology related to real-time control of human specimen fluid exchange

This part analyzes the principle of automatic fluid change in human specimen bottles. A gradient descent algorithm is introduced into the autotuning real-time control system. And further optimize for the limitations of the algorithm by introducing stochastic perturbations.

2.1. Methods of fluid exchange in specimen bottles

2.1.1. Opening method. The method of opening the cap is above the sink, one hand to take the specimen bottle and make it tilted 45 degrees, the other hand with warm water (such as overnight thermos of water) slowly rinse sealing wax on the edge of the bottle mouth, about 1 minute, the bottle mouth has been loosened, with a large mouth pliers gripped the glass sphere on the cap, so that can be opened. For larger specimen bottles can be completed with the collaboration of two people.

2.1.2. Liquid change method. Since formaldehyde is a gas with an irritating odor, this procedure is performed in a fume hood.

Pour the yellowed and turbid liquid in the specimen bottle into the waste liquid tank, and then organize the specimen in the bottle. Such as fixing the specimen of the rope has been loosened to tie up, the specimen posture should be placed to facilitate the observation and so on. After finishing, with a deflector rod to the prepared liquid formaldehyde, glycerol, distilled water into the bottle, the height of the liquid surface to completely submerge the specimen is appropriate, the liquid must not be too full.

2.1.3. Waxing methods. Specimen bottle sealing wax, can be a power of 35W soldering iron energized and heated, and then a hand to take the wax, a hand with the head of the soldering iron pressed against the tip of the wax, along the specimen bottle along the inner mouth together with the uniform speed of movement for a week, the wax will be fast and uniform sealing the bottle mouth. This sealing specimen bottle neat and beautiful.

2.2. Automatic liquid change principle design and material selection

The automatic liquid change device consists of a float valve chamber, a float and a valve movable part connected to the float, a liquid channel (inlet pipe) inserted into the rod, an outlet pipe, an inlet pipe, a handle and other components. Figure 1 is the principle of automatic liquid change device. The working principle is: when the liquid of the previous bag flows into the valve chamber through the inlet tube, the opening of the inlet tube in the valve chamber is larger than the opening of the outlet tube in the valve chamber, thus the valve chamber is full of liquid, when the buoyancy of the float valve is larger than its gravity, the float valve floats up, driving the valve activity part to slide into the valve fixed part and close the valve, realizing that the current soft bottle of liquid infusion waiting for the liquid of the previous bag of liquid to pass through the head of the infusion smoothly. The previous bag of liquid passes through this infusion head smoothly. Similarly, all the soft bags behind are realized infusion waiting. After the infusion of the previous soft bag of liquid air into the valve chamber through the liquid tube, the liquid inside the valve chamber is reduced, the buoyancy force on the float valve is less than its gravity, the float drops, driving the valve connected to the valve activity section slides out of the valve fixed section, the valve is open, then the current soft bag of liquid through the bag of liquid channel flow through the valve into the liquid tube, part of which continues to flow backward, and part of which flows back into the valve chamber. When the liquid flowing into the valve chamber reaches a certain height (when it is about to enter the outlet pipe), the float valve floats up, temporarily interrupts the infusion, and after the liquid level in the valve chamber drops again under the "suction" of the outlet pipe, the float valve sinks again, the valve opens, and the liquid infusion continues, so as

to sink the "pulse" infusion.

In the choice of materials to emphasize two points: ① safety, that is, all plastic molding parts for processing are medical resin processing molding; ② light enough, that is, the float valve materials selected should be as small as possible relative density. Currently all medical polymer materials in the relative density of the smallest is polymethylpentene (relative density of 0.84), followed by linear tri-block copolymer (SEBS), the relative density of 0.92.

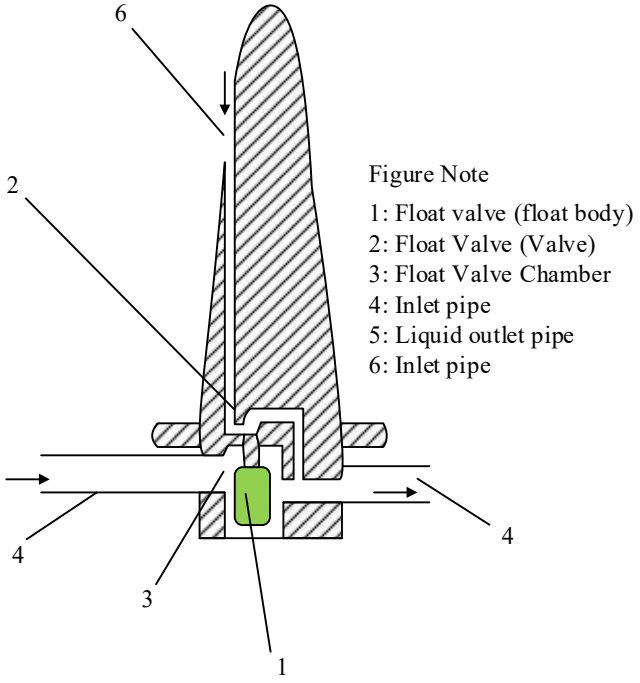

Fig. 1. Principle of automatic liquid changer

2.3. Gradient descent algorithm principle and optimization

The gradient descent algorithm, which is commonly used in neural network optimization problems, is introduced into the automatic fluid exchange system to calculate the changes of human specimen fluids in the process of fluid exchange, so as to realize the real-time control of the steps of fluid exchange, such as “infusion” and “suction”.

Gradient descent is one of the most commonly used optimization methods in neural networks, which mainly includes three algorithms, namely, full gradient descent (FGD), stochastic gradient descent (SGD), and mini-Batch SGD. To facilitate the exposition, the concept of loss function is first introduced. The neural network optimization problem can be described as a minimization problem:

$$\min_{\theta} E(\theta) = \frac{1}{n}\sum_{i=1}^{n} \psi_i\left(y_i, N\left(x_i;\theta\right)\right) \tag{1}$$

where $E(\cdot)$ is the total loss function (objective function) of the neural network, θ denotes the weight parameters to be optimized in the neural network, n is the total number of samples to be observed, ψ_i is the value of the loss function of the ith observation, and $N(\cdot)$ denotes this neural network model.

2.3.1. Full Gradient Descent Algorithm. During the t th iteration, the FGD algorithm uses the entire training dataset to compute the gradient, and the algorithm iteration formula is:

$$\theta_{t+1} = \theta_t - \frac{\eta}{n}\sum_{i=1}^{n}\nabla\psi_i\left(\theta_t\right) \tag{2}$$

Where η denotes the learning rate and $\nabla\psi\left(\theta_t\right)$ is the objective function gradient. Since the gradient needs to be computed using all the samples for each weight update, the FGD algorithm is able to fully reflect the data features and has extremely stable convergence at a suitable learning rate. However, precisely because of the use of full gradient information, the iteration cost is linearly correlated with the dataset size n, so the algorithm is overall slower and has a larger memory overhead, which is not suitable for online, large-scale data.

2.3.2. Stochastic Gradient Descent Algorithm. The SGD algorithm is a variant of the FGD algorithm, with the main difference being the use of a single sample $\left(x_t, y_t\right)$ to update the model parameters at each iteration in order to increase the overall iteration speed of the algorithm, whose iteration formula is:

$$\theta_{t+1} = \theta_t - \eta\nabla\psi\left(\theta_t\right) \tag{3}$$

By comparing the two algorithms mentioned above, it can be seen that the SGD algorithm and the FGD algorithm are two extremes of a series of gradient descent algorithms, corresponding to optimization strategies that use single-sample and full-sample information, respectively, and each possesses its own unique advantages and disadvantages. First, the iterative process of the SGD algorithm uses the gradient of only one sample, so the overall model training is fast. For large-scale datasets, only partial samples are needed to achieve convergence. Also, it is the unique optimization strategy that makes SGD suitable for online learning scenarios, allowing for dynamic updates in real time with the addition of new data. On the other hand, the direction of parameter update in each iteration contains only single sample information and cannot represent the full sample gradient, which leads to randomness in the iteration process; randomly using single sample gradient instead of full sample gradient update also makes the model indirectly learn the sample noise, and the direction of weight update is not always correct. In addition to this, the FGD algorithm is easy to converge to a local optimal solution and the problem of choosing the learning rate has not been solved.

2.3.3. Stochastic Gradient Descent Algorithm for Small Batches. The Mini-BatchSGD algorithm is another variant of the gradient descent method, between the SGD algorithm and the FGD algorithm, and nowadays stochastic gradient descent method generally refers to the Mini-BatchSGD algorithm. In the Mini-BatchSGD algorithm, instead of randomly selecting a single sample or the entire dataset when updating the model parameters in each iteration, a small batch of samples is randomly selected to compute the gradient for parameter updating. This method combines the advantages of the two, which can make full use of the randomness of the samples and reduce the computational overhead.The Mini-BatchSGD algorithm iteration formula is:

$$\theta_{t+1} = \theta_t - \frac{\eta}{batch}\sum_{i=1}^{batch}\nabla\psi_i\left(\theta_t\right) \tag{4}$$

where $batch$ is the size of the randomly selected sample. When $batch = 1$, the Mini-BatchSGD algorithm degenerates into the SGD algorithm; when $batch = n$, the Mini-BatchSGD algorithm transforms into the FGD algorithm. The Mini-BatchSGD algorithm is able to converge to the optimal direction despite the fact that there is some bias between the gradient computed using a small batch of samples and the standard gradient computed using the full sample, resulting in each iteration not going in the direction of the fastest decrease in the value of the loss function. In addition, this gradient bias introduces a small amount of noise to the samples, which improves the generalization ability of the model to some extent.

2.3.4. SPGD algorithm principle and workflow. The gradient descent algorithm is optimized for the human specimen fluid exchange process, which has more control variables, the controlled system is complex and an accurate mathematical model cannot be established, and the gradient descent algorithm has limitations such as the bias in sample calculation.The SPGD algorithm is an optimization algorithm after applying stochastic perturbations to all the control parameters of the objective function of the SGD algorithm, and it is able to more accurately achieve the human body fluid exchange process in the real-time regulation and control and reduce the possible errors.

The basic principle of the SPGD algorithm is to calculate the gradient change of the evaluation function after perturbation by randomly perturbing multiple control variables in parallel. Then, according to the changes in the gradient of the evaluation function before and after the perturbation, feedback control of the control variables is carried out, so that the gradient of the evaluation function is continuously reduced, thus gradually making the evaluation function value reach the extreme value.The SPGD algorithm utilizes the gradient information to guide the updating of the parameters, so as to achieve the iteration of the optimization process until the stopping condition is satisfied. Due to its parallel control characteristics, the SPGD algorithm is suitable for optimization control processes with multiple control variables. Its feedback evaluation criterion based on gradient descent makes it unnecessary to pay attention to the specific system mathematical model, so the SPGD algorithm is widely applicable to the optimal control process where the controlled system is more complex and an accurate mathematical model cannot be established.The principle of the SPGD algorithm is as follows:

J denotes the system evaluation function, u_N denotes the N road control voltage, and δu_N denotes the randomized perturbation voltage, then the variation of the system performance evaluation function is as follows:

$$\delta J = J\left(u_1 + \delta u_1, u_2 + \delta u_2 \cdots u_N + \delta u_N\right) - J\left(u_1, \cdots u_N\right) \tag{5}$$

After obtaining the performance evaluation function of the system, the control voltage is updated as $u_{(N+1)}$ and the control voltage of the jth channel according to the gradient descent formula can be written as:

$$u_j^{(n+1)} = u_j^{(n)} - \lambda \nabla J_j\left(u_1^{(n)}, \cdots, u_N^{(n)}\right), j = 1, \cdots, N \tag{6}$$

where $\nabla J_j\left(u_1^{(n)}, \ldots, u_N^{(n)}\right)$ denotes the gradient of the system's performance evaluation function, and λ denotes the iteration step size. Taylor expansion of (5) yields:

$$\delta J = \sum_j^N \frac{\partial J}{\partial u_j} \delta u_j + \frac{1}{2} \sum_{j,k=1}^N \frac{\partial^2 J}{\delta u_j \delta u_k} \delta u_j \delta u_k + \cdots \tag{7}$$

Multiplying both sides of the above equation simultaneously by δu_i gives:

$$\delta J \delta u_i = \sum_j^N \frac{\partial J}{\partial u_j} \left(\delta u_j \delta u_i\right) + \frac{1}{2} \sum_{j,k}^N \frac{\partial^2 J}{\delta u_j \delta u_k} \delta u_j \delta u_k \delta u_i + \cdots \tag{8}$$

The generated random perturbations $\delta u = \left\{\delta u_1, \ldots, \delta u_N\right\}$ obey a Bernoulli distribution obtained from knowledge of probability theory:

$$\left\langle \delta u_i \right\rangle = 0, \left\langle \delta u_i \delta u_j \right\rangle = \delta^2 \delta_{ij} \tag{9}$$

where δ^2 denotes the variance of the random perturbation. The second term in Eq. (8) is zero in the mean sense and can be written:

$$\left\langle \delta J \delta u_i \right\rangle = \frac{\partial J}{\partial_{u_j}} \delta^2 + o\left(\delta^4\right) \tag{10}$$

Dividing both sides of (10) simultaneously by δ^2 gives:

$$\frac{\partial J}{\partial u_j} = \frac{\langle \delta J \delta u_i \rangle}{\delta^2} - o\left(\delta^2\right) \tag{11}$$

Ignoring the second higher order minor, substituting (11) into (6) yields:

$$u_j^{(n+1)} = u_j^{(n)} - \gamma \delta J^{(n)} \delta u_j^{(n)}, j = 1, \ldots, N \tag{12}$$

The above equation is the iterative formula for the stochastic parallel gradient descent algorithm, where

$$\gamma = \frac{\lambda}{\delta^2} \tag{13}$$

Then the stochastic parallel gradient descent algorithm iteration formula is:

$$u^{(n+1)} = u^{(n)} - \gamma \delta J^{(n)} \delta u^{(n)} \tag{14}$$

The flow of stochastic parallel gradient descent algorithm based on energy feedback is as follows:

1) Set the initial energy threshold;

2) Set the initial voltage usually set it as a set of zero vectors, or choose a set of values closer to the extremes according to practical needs;

3) Generate a set of randomly perturbed voltages $\delta u = \{\delta u_1, \delta u_2, \ldots, \delta u_N\}$ obeying a Bernoulli distribution;

4) Apply a forward perturbation signal $u^+ = u^n + \delta u$ to the fast mirror to get the performance index of the system at this time $J\left(u^+\right)$, and then apply a reverse perturbation voltage $u^- = u^n - \delta u$ to the fast mirror to get the performance index of the system at this time $J\left(u^-\right)$;

5) Get the amount of indicator change of the system $\delta J = J\left(u^+\right) - J\left(u^-\right)$;

6) Substitute the amount of change in the indicators of the system into the iterative formula (14) to update the control voltage applied to the fastback mirror;

7) Detect whether the final correction result has been reached, if the correction has been completed, jump out of the execution, if the correction requirements have not been met, jump to step 3 to continue to run until the completion of the correction or the set number of iteration steps to complete the iteration.

The SPGD algorithm is superior to other algorithms in the incoherent beam combining, but the SPGD algorithm also has certain defects, which can be seen through Eq. (14), and the selection of the parameters of the SPGD algorithm affects the convergence speed of the algorithm as well as the convergence accuracy.

3. Validation of the effect of real-time control of fluid exchange in human specimens

This chapter constructs a sample set of liquid concentration and real-time power control for the SPGD algorithm to provide learning data for the SPGD algorithm. The performance advantages of the SPGD algorithm are investigated through simulation experiments. Verify the relative error and repeatability deviation of the real-time control system introducing SPGD algorithm in the liquid pipetting process, and judge its application value in the actual specimen liquid exchange process.

3.1. Design of real-time power control scheme for specimen fluid exchange

3.1.1. Real-time power-controlled sample set creation for specimen fluid exchange. There are many parameters involved in the real-time control process of human specimen liquid exchange, in this paper, we mainly choose the product of surface tension and viscosity of different liquid concentrations and real-time power of liquid exchange as the research object of SPGD algorithm. First of all, it is necessary to establish the sample set of liquid concentration and real-time power of specimen liquid exchange, so as to facilitate the subsequent learning and calculation using the SPGD algorithm.

Studying the fitted linear equations of different concentrations of human specimen liquids in specimen bottles during the liquid exchange process, it can be seen that, with the decrease of the proportion of liquids, the slope of the fitted linear equations decreases from 1.12645 to 0.58697, and the intercepts with the vertical coordinates increase from -1.46508 to -0.98144, and all of them have a very strong linear correlation (the minimum of R^2 is 0.978). This shows on the one hand that there is indeed a linear correlation between the liquid change speed and the input power; on the other hand, it also proves that different concentrations of liquids have different values of surface tension and viscosity product, and liquids with different values of surface tension and viscosity product have different linear relationships, and the larger the surface tension and viscosity product, the smaller the slope of the fitted linear equation and the larger the intercept with the vertical coordinate.

After obtaining the relationship between the liquid change speed and input power of different concentration of specimen liquids by calculation, the input power of different concentration liquids at any one liquid change speed can be calculated by using the fitted linear equation, which can provide the basic data for the subsequent learning of the sample set of SPGD algorithm. Six velocity points, 0.4 m/s, 0.5 m/s, 0.6 m/s, 0.7 m/s, 0.8 m/s, 0.9 m/s, were selected, and the input powers corresponding to these six velocity points were calculated when liquid exchange was performed on liquids of different concentrations. Different concentrations of specimen liquids all correspond to a different product of surface tension and viscosity. Table 1 shows the speed and power calculations corresponding to each of the five different surface tension and viscosity products. For example, the fitted linear equation for 75% human specimen liquid (corresponding to a surface tension and viscosity product value of 195.4798N2·s/m3) is y=0.58693x-0.98140, and substituting 0.4m/s into the equation can be calculated to obtain the corresponding input power of 2.3536mW, and similarly, substituting 0.5m/s, 0.6m /s, 0.7m/s, 0.8m/s and 0.9m/s into the equation can be calculated to obtain the corresponding input power of 2.3536mW, 2.5240mW, 2.6944mW, 2.8647mW and 3.2055mW respectively.

Table 1. Speed and power of different surface tension and viscosity

Surface tension × viscosity (N2·s/m3)	Power at 0.4m/s (mW)	Power at 0.5m/s (mW)	Power at 0.6m/s (mW)	Power at 0.7m/s (mW)	Power at 0.8m/s (mW)	Power at 0.9m/s (mW)
195.4798	2.3536	2.5240	2.6944	2.8647	3.0351	3.2055
165.3894	2.1718	2.3187	2.4660	2.6132	2.7601	3.1024
136.4051	1.9285	2.0465	2.1641	2.2871	2.4100	3.2006
114.7561	1.8096	1.9177	2.0264	2.1348	2.2430	2.7127
85.08359	1.6558	1.7444	1.8336	1.921	2.0107	2.3130

Based on the data in Table 1 a linear fit can be made to the surface tension × viscosity and the input power at the same fluid change speed. For example, at a detachment speed of 0.4 m/s, the input power corresponding to liquids with surface tension × viscosity of 195.4798, 165.3894, 136.4051, 114.7561, and 85.0839N2·s/m3 are 2.3536, 2.1718, 1.9285, and 1.8096, respectively, 1.6558 mW. Linear fitting was performed to find the corresponding fitted linear equations. The linear equations were plotted against the input power for different surface tension and viscosity products as a sample set for real-time power control.

Figure 2 demonstrates the relationship between the fluid exchange velocity and input power for different surface tension and viscosity products. As can be seen from Fig. 2, the fitted linear equations of surface tension × viscosity and input power corresponding to the six velocity points have excellent linear correlation and show a good pattern: the slope of the fitted straight line increases from 0.00648 to 0.00785 as the velocity increases from 0.4 m/s to 0.9 m/s, and the intercept from the vertical coordinate increases from 1.07981 to 1.81230. This indicates that the that it is reasonable to use the product of surface tension and viscosity as a characteristic parameter in this paper to investigate the input power at specific velocities for liquids of different concentrations. This power control sample set has the following functions: 1) for the existing velocity points in the sample set, the input power corresponding to any reagent with surface tension and viscosity product at this velocity point is given; 2) for a specific reagent with surface tension and viscosity product, the input power corresponding to the six velocity points of this reagent is obtained by calculating six linear equations in the sample set, and the input powers corresponding to the six velocity points of this reagent can be obtained by using these six velocity points and the corresponding input powers. Using these six velocity points and the corresponding input powers, a linear equation can be fitted and used to calculate the input power corresponding to any detachment velocity for this reagent.

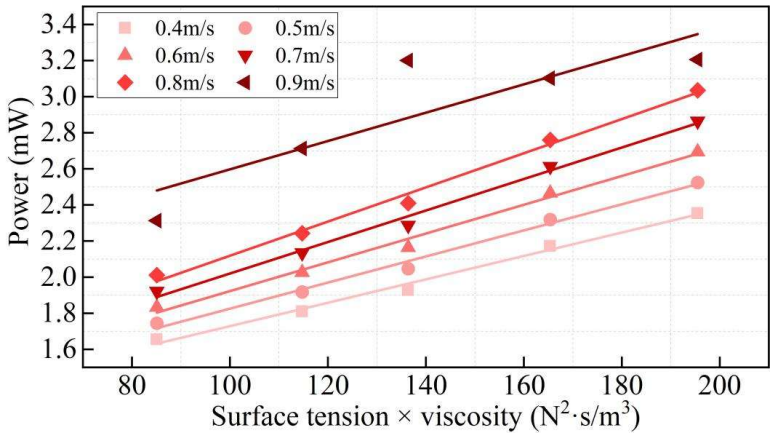

Fig. 2. Infusion speed and input power under different product

3.1.2. Validation of the sample set based power real-time control scheme. The power control sample set was validated using the surface tension × viscosity reference values for the three concentration specimen liquids and one of the measurements. The input power corresponding to each velocity point for each reagent can be calculated from Figure 2.

The 75% concentration specimen liquid is used as an example to illustrate the calculation of the input power corresponding to each velocity point as follows: the reference value of the surface tension x viscosity of the 75% concentration specimen liquid is 185.1548N2·s/m3, and the measured value is 181.715N2·s/m3, which is respectively substituted into the fitting of 0.4m/s in Figure 2 The linear equation y=0.00648x+1.07981 was used to obtain the input power for the reference and measured values, respectively. The droplets were excited five times for 75% liquid concentration with each input power value to obtain their true velocities. Figure 3 shows the velocity results obtained by exciting 75% liquid concentration with each input power value. Each input power corresponds to an expected excitation droplet velocity, referred to in this paper as the set velocity value, which is indicated by dark red rectangular dots in Figure 3. The mid-red circular dots are the velocities obtained by exciting the droplets using the input power corresponding to the surface tension × viscosity reference value, and the light red triangles are the velocities obtained by exciting the droplets using the input power corresponding to the surface tension × viscosity measurement value. The linear equation fitted to the set velocity value is: y=0.58298x-0.78588 (R^2=0.998); the linear equation fitted to the velocity of the droplet excited by the power of the reference value is: y=0.58508x-0.77297 (R^2=0.994); the linear equation fitted to the velocity of the droplet excited by the power of the measured value is: y=0.57670x-0.75185 (R^2=0.990). 0.990).

By analogy, the real-time infusion power of liquids of different concentrations during fluid exchange can be calculated by learning and utilizing the fitted linear equations of the power control sample set to achieve the regulation of the concentration and power parameters.

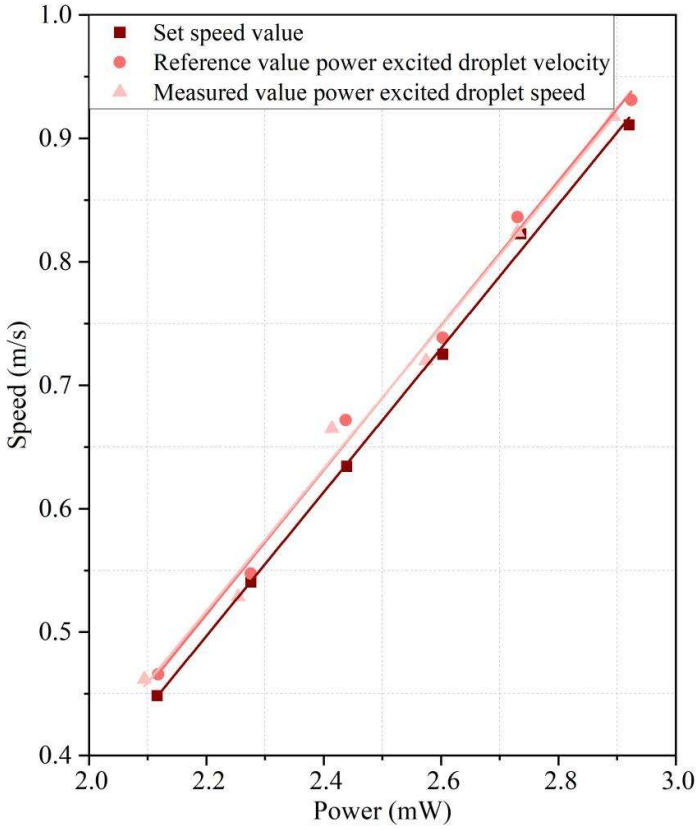

Fig. 3. Velocity obtained from 75% concentration excited by the input power

3.2. Simulation experiments of the algorithm before and after optimization

In order to judge the performance advantage of the SPGD algorithm after adding random perturbation voltage and to verify its optimization effect of fluid exchange in real-time automatic control system, numerical simulation is used to simulate and compare and analyze the traditional SGD algorithm and the optimized SPGD algorithm respectively. The traditional SGD algorithm searches for the optimal step size through several experiments, while the optimized SPGD algorithm randomly selects the step size in the convergence interval. In the simulation process of SPGD algorithm, Ux, N and Uy, N are used to denote the voltage values of the Nth laser in the x and y directions, and the bilateral perturbation method is adopted, the perturbation voltage Uδ obeys the Bernoulli distribution, and the PIB evaluation function value is used to denote the convergence accuracy.

3.2.1. Analysis of simulation results. The traditional SGD algorithm and the optimized SPGD algorithm with the addition of random perturbation voltage are simulated for the human specimen fluid exchange process respectively, and 150 iterations of experiments are performed for both algorithms. Figure 4 shows the 150 experimental iteration curves of the optimized SPGD algorithm (the first 15 times are shown as a demonstration). Figure 5 shows the evaluation function values before and after adding the random perturbation voltage. The evaluation function value reaches 0.92 when the traditional algorithm is iterated up to 20 times; the improved algorithm reaches 0.92 when iterated up to 14 times. Compared with the two, the speed of the improved algorithm is increased by 30%. After 150 iterations, the power of the traditional SGD algorithm reaches 3m/W and the power of the improved SPGD algorithm reaches 5m/W. The convergence of the improved SPGD algorithm is improved.

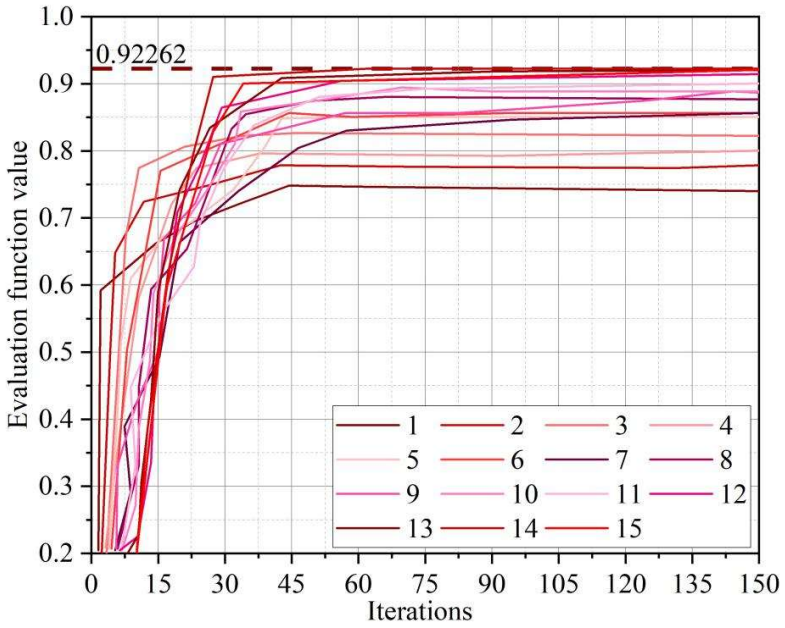

Fig. 4. SPGD's 150 experimental iterations curve (Top15)

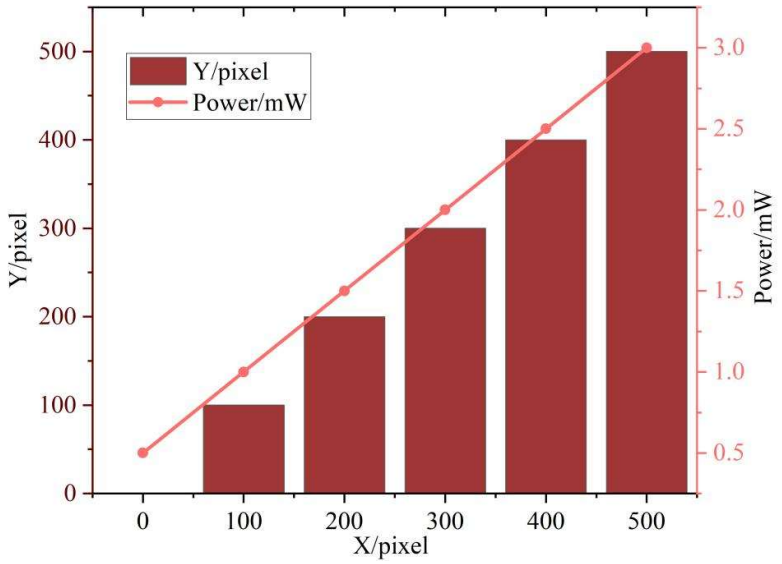

(a) Traditional SGD power variation

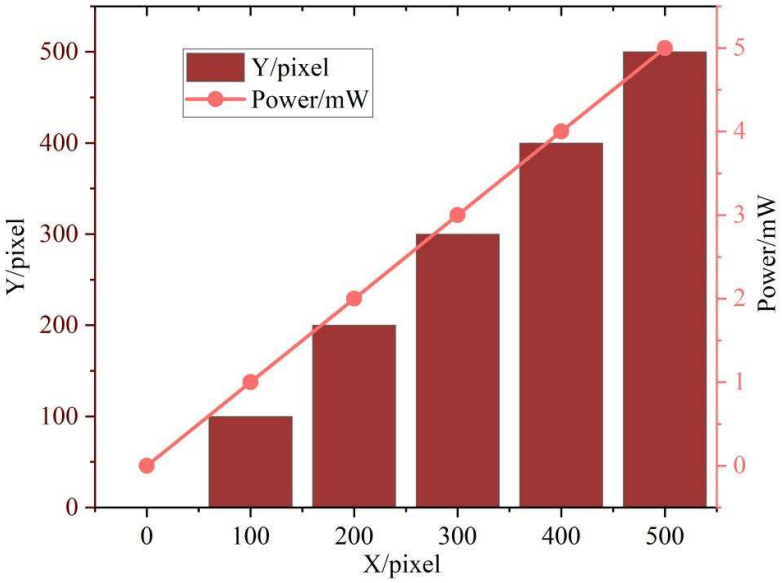

(b) Optimize SPGD power variation

Fig. 5. Power change before and after adding random disturbance voltage

3.2.2. Iterative optimization experiments. According to the experimental procedure of 3.2.1, 15 repetitions of the traditional SGD algorithm and the improved SPGD algorithm are performed respectively, and the data of the 15 experiments are averaged. Figure 6 shows the average convergence curves of the two algorithms. From Fig. 6, it can be seen that the evaluation function value of the traditional SGD algorithm reaches 0.81 at 45 iterations, and the convergence accuracy reaches 0.9297 at the end of 150 iterations; whereas the evaluation function value of the improved SPGD algorithm reaches 0.83 at only 31 iterations, and the convergence accuracy reaches 0.9698 at the end of 150 iterations. it can be seen from the results of multiple experiments that the convergence speed and convergence accuracy is better than that of the traditional SGD algorithm, and the improved SPGD algorithm can more quickly and accurately calculate the changes in the values of the parameters such as liquid concentration and input power during the liquid exchange of the human specimen, which in turn provides more effective support for real-time control.

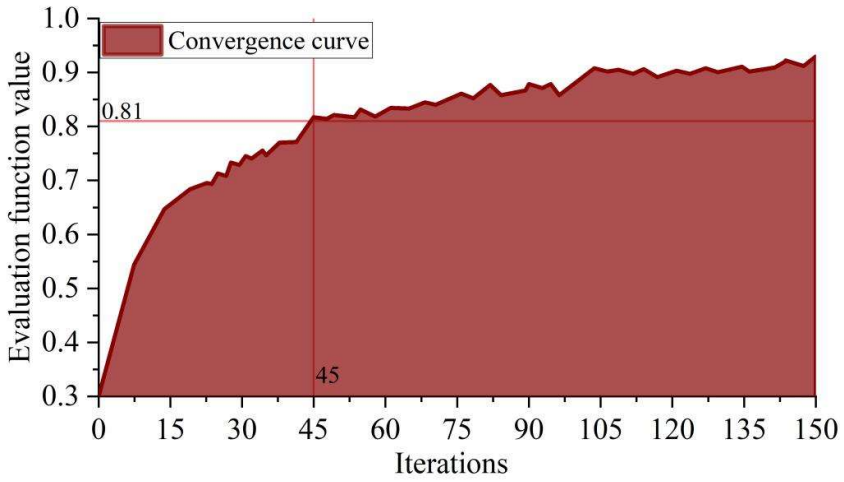

(a) Taditional SGD algorithm

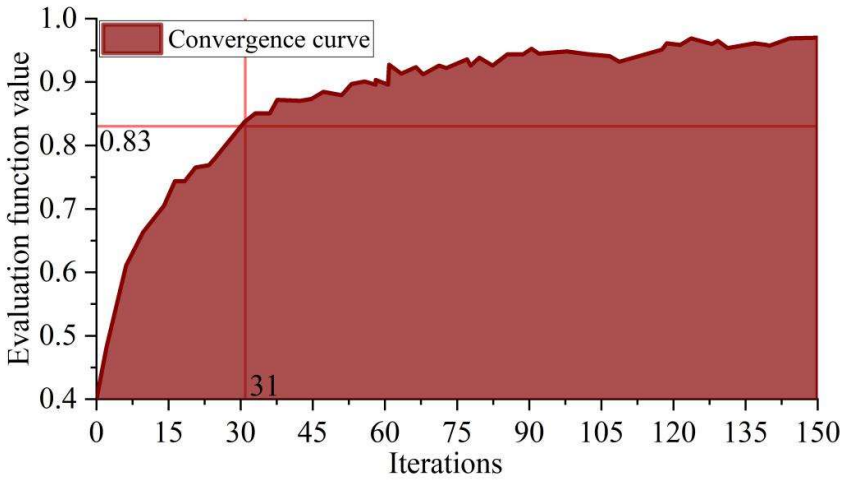

(a) Improved SPGD algorithm

Fig. 6. The average convergence curve of the two algorithms

3.3. Validation of Relative Error and Repeatability Deviation of Liquid Pipetting Processes

When the liquid flowing into the valve chamber reaches a certain height, the automatic fluid exchange system will have a pause infusion, waiting for the infusion tube "suction" process. For this "suction" (i.e., "pipetting") process in the liquid exchange process, the relative error and repeatability deviation of the improved SPGD algorithm are verified, and it is judged whether the calculation error meets the requirements of the national metrology and testing regulations. According to the national metrological testing regulations of pipettes for the metrological performance of pipetting process, the allowable error of the pipette volume at room temperature 25℃ for a standard volume of 250 μl is not more than 1.5%, and the repeatability deviation of the measurement is not more than 1%.

Table 2 shows the average value, relative error value and repeatability deviation of the pipetting data of 4 groups of different capacities calculated by the improved SPGD algorithm. From Table 2, it can be seen that the relative error of pipetting for the 4 groups of different volumes does not exceed 1.5% and the repeatability deviation is less than 1%. Comparing the relative errors and repeatability deviations of different pipetting data in Table 2 with the permissible range of standard parameter errors, it can be seen that the pipetting results of introducing the improved SPGD algorithm for pipetting operation experiments in the automatic liquid exchange system are in line with the national metrological testing regulations.

Table 2. Calculation results

Set capacity/μl	75	150	225	250
Mean value $\tilde{V}$/μl	48.8015	97.8181	147.463	196.890
Relative error E/%	1.221	1.342	1.230	1.141
Repeatability deviation CV/%	0.901	0.802	0.355	0.413

3.4. Practical application of real-time control system for automatic liquid change

Introducing the improved SPGD algorithm in the real-time control system for human specimen liquid exchange can effectively control the liquid concentration and real-time power during specimen liquid exchange, and the error generated in the pipetting process is small. The human specimen liquid exchange experiment is carried out in the real-time control system introducing the improved SPGD algorithm to verify its effect in the application of actual specimen liquid exchange. Prepare the corresponding specimen bottles and materials according to the methods of 2.1 and 2.2 for the preexperiment preparation.

Figure 7 shows the real-time monitoring curve of power during the liquid exchange process. The horizontal coordinate represents the time when the liquid exchange process occurred, and the vertical coordinate represents the power output after the system real-time concentration in the specimen bottle. From the liquid exchange process in Fig. 7, it can be seen that in the time range of 0-120ms, the concentration of the liquid in the specimen bottle changes continuously due to the steps of liquid in, suction, and liquid out as the time of liquid exchange passes. In the real-time control system that introduces the improved SPGD algorithm, the corresponding system output power (between 2mW-4mW) is continuously given according to the change of the liquid concentration in the specimen bottle to guide the liquid exchange behavior at the next time point, which makes the whole process of liquid exchange to be carried out in a stable manner, and reduces the possibility of damage to the human specimen.

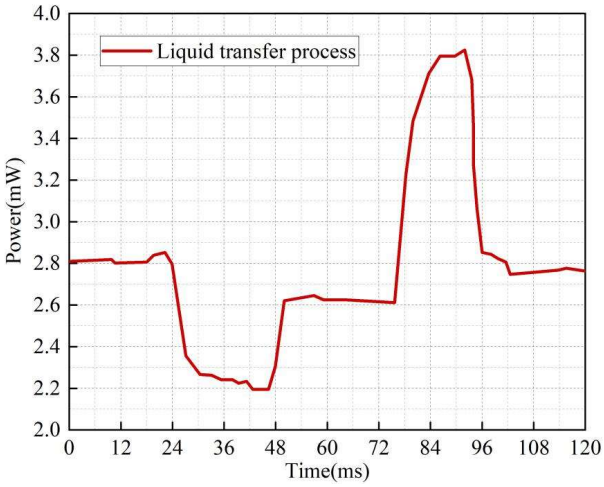

Fig. 7. Real-time power monitoring curve during liquid change

4. Conclusion

In this paper, the optimized SPGD algorithm is introduced into the real-time control system for human specimen fluid exchange to realize the real-time monitoring of specimen bottle liquid concentration and power of fluid exchange during the process of fluid exchange and to maintain a smooth fluid exchange speed. By constructing the sample set of real-time concentration and power of specimen

liquid exchange, data support is provided to reduce the computational volume of SPGD algorithm and improve the accuracy of subsequent monitoring. In simulation experiments, the optimized SPGD algorithm evaluation function value reaches 0.83 with only 31 iterations, and the convergence accuracy reaches 0.9698 at the end of 150 iterations, which has higher convergence accuracy and faster convergence effect. The error and repeatability deviation of the pipetting step do not exceed 1.5% and 1% of the national measurement and testing regulations. And in the actual liquid exchange experiments, it can smoothly output the changing relationship between liquid concentration and liquid exchange power to realize the real-time regulation of liquid exchange speed. The introduction of SPGD algorithm to optimize the real-time control system of human specimen liquid exchange under the adaptive regulation mode can control the operation speed in the liquid exchange process more quickly and accurately, reduce the cost of liquid exchange, and reduce the risk of damage to the human specimen due to liquid exchange. After that, the calculation precision of the algorithm can be further improved to realize the simultaneous operation of multiple human specimen fluid exchange and save the cost of fluid exchange.

Acknowledgements

Shandong Yingcai University's university-level research project, Research on the Design of a Collection Device for Human Anatomy Specimens (YCKY22012).

References

[1] Obando, F. D. C., & Rueda-Esteban, R. J. (2020). Formolized Cadaveric Specimens Immersion-Recovery Protocol. The FASEB Journal, 34(S1), 1-1.

[2] Friend, P. J. (2020). Strategies in organ preservation—a new golden age. Transplantation, 104(9), 1753-1755.

[3] Jing, L., Konoeda, H., Keshavjee, S., & Liu, M. (2021). Using nutrient-rich solutions and adding multiple cytoprotective agents as new strategies to develop lung preservation solutions. American Journal of Physiology-Lung Cellular and Molecular Physiology, 320(6), L979-L989.

[4] Garrood, M., Thorn, E. L., Goldstein, A., Sowa, A., Janssen, W., Wilson, A., ... & McKenzie, A. T. (2025). Preservation of cellular structure via immersion fixation in brain banking. Free Neuropathology, 6, 4.

[5] Dakappagari, N., Zhang, H., Stephen, L., Amaravadi, L., & Khan, M. U. (2017). Recommendations for clinical biomarker specimen preservation and stability assessments. Bioanalysis, 9(8), 643-653.

[6] Tamayo-Arango, L., & Garzón-Alzate, A. (2018). Preservation of animal cadavers with a formaldehyde-free solution for gross anatomy. Journal of Morphological Sciences, 35(02), 136-141.

[7] Jing, L., Yao, L., Zhao, M., Peng, L. P., & Liu, M. (2018). Organ preservation: from the past to the future. Acta Pharmacologica Sinica, 39(5), 845-857.

[8] Domański, J., Janczura, A., Wanat, M., Wiglusz, K., Grajzer, M., Simmons, J. E., ... & Szepietowski, J. C. (2023). Preservation fluids of heritage anatomical specimens—a challenge for modern science. Studies of the origin, composition and microbiological contamination of old museum collections. Journal of Anatomy, 243(1), 148-166.

[9] Ostróżka-Cieślik, A., Dolińska, B., & Ryszka, F. (2018). Tips for optimizing organ preservation solutions. Acta Biochimica Polonica, 65(1), 9-15.

[10] Gonzalez, J. M., Villarreal, C., Fasci, A., Rocco, D. D., Salazar, S., Khalil, A., ... & Hood, R. L. (2022). Evaluating the performance of a nonelectronic, versatile oxygenating perfusion system across viscosities representative of clinical perfusion solutions used for organ preservation. Bioengineering, 10(1), 2.

[11] Haji, S. H., & Abdulazeez, A. M. (2021). Comparison of optimization techniques based on gradient descent algorithm: A review. PalArch's Journal of Archaeology of Egypt/Egyptology, 18(4), 2715-2743.

[12] Yi, D., Ji, S., & Bu, S. (2019). An enhanced optimization scheme based on gradient descent methods for machine learning. Symmetry, 11(7), 942.

[13] Tian, Y., Zhang, Y., & Zhang, H. (2023). Recent advances in stochastic gradient descent in deep learning. Mathematics, 11(3), 682.

[14] Lyu, F., Xu, X., & Zha, X. (2022). An adaptive gradient descent attitude estimation algorithm based on a fuzzy system for UUVs. Ocean Engineering, 266, 113025.

[15] Ali, M., & AbouRizk, S. (2024). Updating simulation model parameters using stochastic gradient descent. Automation in Construction, 166, 105676.